2009

Angular distributions in the decay B -> K*l(+)l(-)

BABAR Collaboration

Recommended Citation

BABAR Collaboration, "Angular distributions in the decay B -> K*l(+)l(-)" (2009). *Physical Review D*. 687.
https://doi.org/10.1103/PhysRevD.79.031102

PHYSICAL REVIEW D **79,** 031102(R) (2009)

Angular distributions in the decay $B \to K^* l^+ l^-$

B. Aubert,[1] M. Bona,[1] Y. Karyotakis,[1] J. P. Lees,[1] V. Poireau,[1] X. Prudent,[1] V. Tisserand,[1] A. Zghiche,[1] J. Garra Tico,[2] E. Grauges,[2] L. Lopez,[3] A. Palano,[3] M. Pappagallo,[3] G. Eigen,[4] B. Stugu,[4] L. Sun,[4] G. S. Abrams,[5] M. Battaglia,[5] D. N. Brown,[5] J. Button-Shafer,[5] R. N. Cahn,[5] R. G. Jacobsen,[5] J. A. Kadyk,[5] L. T. Kerth,[5] Yu. G. Kolomensky,[5] G. Kukartsev,[5] G. Lynch,[5] I. L. Osipenkov,[5] M. T. Ronan,[5,*] K. Tackmann,[5] T. Tanabe,[5] W. A. Wenzel,[5] C. M. Hawkes,[6] N. Soni,[6] A. T. Watson,[6] H. Koch,[7] T. Schroeder,[7] D. Walker,[8] D. J. Asgeirsson,[9] T. Cuhadar-Donszelmann,[9] B. G. Fulsom,[9] C. Hearty,[9] T. S. Mattison,[9] J. A. McKenna,[9] M. Barrett,[10] A. Khan,[10] M. Saleem,[10] L. Teodorescu,[10] V. E. Blinov,[11] A. D. Bukin,[11] A. R. Buzykaev,[11] V. P. Druzhinin,[11] V. B. Golubev,[11] A. P. Onuchin,[11] S. I. Serednyakov,[11] Yu. I. Skovpen,[11] E. P. Solodov,[11] K. Yu. Todyshev,[11] M. Bondioli,[12] S. Curry,[12] I. Eschrich,[12] D. Kirkby,[12] A. J. Lankford,[12] P. Lund,[12] M. Mandelkern,[12] E. C. Martin,[12] D. P. Stoker,[12] S. Abachi,[13] C. Buchanan,[13] J. W. Gary,[14] F. Liu,[14] O. Long,[14] B. C. Shen,[14,*] G. M. Vitug,[14] Z. Yasin,[14] L. Zhang,[14] V. Sharma,[15] C. Campagnari,[16] T. M. Hong,[16] D. Kovalskyi,[16] M. A. Mazur,[16] J. D. Richman,[16] T. W. Beck,[17] A. M. Eisner,[17] C. J. Flacco,[17] C. A. Heusch,[17] J. Kroseberg,[17] W. S. Lockman,[17] T. Schalk,[17] B. A. Schumm,[17] A. Seiden,[17] L. Wang,[17] M. G. Wilson,[17] L. O. Winstrom,[17] C. H. Cheng,[18] D. A. Doll,[18] B. Echenard,[18] F. Fang,[18] D. G. Hitlin,[18] I. Narsky,[18] T. Piatenko,[18] F. C. Porter,[18] R. Andreassen,[19] G. Mancinelli,[19] B. T. Meadows,[19] K. Mishra,[19] M. D. Sokoloff,[19] F. Blanc,[20] P. C. Bloom,[20] W. T. Ford,[20] J. F. Hirschauer,[20] A. Kreisel,[20] M. Nagel,[20] U. Nauenberg,[20] A. Olivas,[20] J. G. Smith,[20] K. A. Ulmer,[20] S. R. Wagner,[20] R. Ayad,[21,†] A. M. Gabareen,[21] A. Soffer,[21,‡] W. H. Toki,[21] R. J. Wilson,[21] D. D. Altenburg,[22] E. Feltresi,[22] A. Hauke,[22] H. Jasper,[22] M. Karbach,[22] J. Merkel,[22] A. Petzold,[22] B. Spaan,[22] K. Wacker,[22] V. Klose,[23] M. J. Kobel,[23] H. M. Lacker,[23] W. F. Mader,[23] R. Nogowski,[23] J. Schubert,[23] K. R. Schubert,[23] R. Schwierz,[23] J. E. Sundermann,[23] A. Volk,[23] D. Bernard,[24] G. R. Bonneaud,[24] E. Latour,[24] Ch. Thiebaux,[24] M. Verderi,[24] P. J. Clark,[25] W. Gradl,[25] S. Playfer,[25] A. I. Robertson,[25] J. E. Watson,[25] M. Andreotti,[26] D. Bettoni,[26] C. Bozzi,[26] R. Calabrese,[26] A. Cecchi,[26] G. Cibinetto,[26] P. Franchini,[26] E. Luppi,[26] M. Negrini,[26] A. Petrella,[26] L. Piemontese,[26] E. Prencipe,[26] V. Santoro,[26] F. Anulli,[27] R. Baldini-Ferroli,[27] A. Calcaterra,[27] R. de Sangro,[27] G. Finocchiaro,[27] S. Pacetti,[27] P. Patteri,[27] I. M. Peruzzi,[27,§] M. Piccolo,[27] M. Rama,[27] A. Zallo,[27] A. Buzzo,[28] R. Contri,[28] M. Lo Vetere,[28] M. M. Macri,[28] M. R. Monge,[28] S. Passaggio,[28] C. Patrignani,[28] E. Robutti,[28] A. Santroni,[28] S. Tosi,[28] K. S. Chaisanguanthum,[29] M. Morii,[29] R. S. Dubitzky,[30] J. Marks,[30] S. Schenk,[30] U. Uwer,[30] D. J. Bard,[31] P. D. Dauncey,[31] J. A. Nash,[31] W. Panduro Vazquez,[31] M. Tibbetts,[31] P. K. Behera,[32] X. Chai,[32] M. J. Charles,[32] U. Mallik,[32] J. Cochran,[33] H. B. Crawley,[33] L. Dong,[33] W. T. Meyer,[33] S. Prell,[33] E. I. Rosenberg,[33] A. E. Rubin,[33] Y. Y. Gao,[34] A. V. Gritsan,[34] Z. J. Guo,[34] C. K. Lae,[34] A. G. Denig,[35] M. Fritsch,[35] G. Schott,[35] N. Arnaud,[36] J. Béquilleux,[36] A. D'Orazio,[36] M. Davier,[36] J. Firmino da Costa,[36] G. Grosdidier,[36] A. Höcker,[36] V. Lepeltier,[36] F. Le Diberder,[36] A. M. Lutz,[36] S. Pruvot,[36] P. Roudeau,[36] M. H. Schune,[36] J. Serrano,[36] V. Sordini,[36] A. Stocchi,[36] W. F. Wang,[36] G. Wormser,[36] D. J. Lange,[37] D. M. Wright,[37] I. Bingham,[38] J. P. Burke,[38] C. A. Chavez,[38] J. R. Fry,[38] E. Gabathuler,[38] R. Gamet,[38] D. E. Hutchcroft,[38] D. J. Payne,[38] C. Touramanis,[38] A. J. Bevan,[39] K. A. George,[39] F. Di Lodovico,[39] R. Sacco,[39] M. Sigamani,[39] G. Cowan,[40] H. U. Flaecher,[40] D. A. Hopkins,[40] S. Paramesvaran,[40] F. Salvatore,[40] A. C. Wren,[40] D. N. Brown,[41] C. L. Davis,[41] K. E. Alwyn,[42] N. R. Barlow,[42] R. J. Barlow,[42] Y. M. Chia,[42] C. L. Edgar,[42] G. D. Lafferty,[42] T. J. West,[42] J. I. Yi,[42] J. Anderson,[43] C. Chen,[43] A. Jawahery,[43] D. A. Roberts,[43] G. Simi,[43] J. M. Tuggle,[43] C. Dallapiccola,[44] S. S. Hertzbach,[44] X. Li,[44] E. Salvati,[44] S. Saremi,[44] R. Cowan,[45] D. Dujmic,[45] P. H. Fisher,[45] K. Koeneke,[45] G. Sciolla,[45] M. Spitznagel,[45] F. Taylor,[45] R. K. Yamamoto,[45] M. Zhao,[45] S. E. Mclachlin,[46,*] P. M. Patel,[46] S. H. Robertson,[46] A. Lazzaro,[47] V. Lombardo,[47] F. Palombo,[47] J. M. Bauer,[48] L. Cremaldi,[48] V. Eschenburg,[48] R. Godang,[48] R. Kroeger,[48] D. A. Sanders,[48] D. J. Summers,[48] H. W. Zhao,[48] S. Brunet,[49] D. Côté,[49] M. Simard,[49] P. Taras,[49] F. B. Viaud,[49] H. Nicholson,[50] G. De Nardo,[51] L. Lista,[51] D. Monorchio,[51] C. Sciacca,[51] M. A. Baak,[52] G. Raven,[52] H. L. Snoek,[52] C. P. Jessop,[53] K. J. Knoepfel,[53] J. M. LoSecco,[53] G. Benelli,[54] L. A. Corwin,[54] K. Honscheid,[54] H. Kagan,[54] R. Kass,[54] J. P. Morris,[54] A. M. Rahimi,[54] J. J. Regensburger,[54] S. J. Sekula,[54] Q. K. Wong,[54] N. L. Blount,[55] J. Brau,[55] R. Frey,[55] O. Igonkina,[55] J. A. Kolb,[55] M. Lu,[55] R. Rahmat,[55] N. B. Sinev,[55] D. Strom,[55] J. Strube,[55] E. Torrence,[55] G. Castelli,[56] N. Gagliardi,[56] A. Gaz,[56] M. Margoni,[56] M. Morandin,[56] M. Posocco,[56] M. Rotondo,[56] F. Simonetto,[56] R. Stroili,[56] C. Voci,[56] P. del Amo Sanchez,[57] E. Ben-Haim,[57] H. Briand,[57] G. Calderini,[57] J. Chauveau,[57] P. David,[57] L. Del Buono,[57] O. Hamon,[57] Ph. Leruste,[57] J. Ocariz,[57] A. Perez,[57] J. Prendki,[57] L. Gladney,[58] M. Biasini,[59] R. Covarelli,[59] E. Manoni,[59] C. Angelini,[60] G. Batignani,[60] S. Bettarini,[60] M. Carpinelli,[60,‖] A. Cervelli,[60] F. Forti,[60] M. A. Giorgi,[60] A. Lusiani,[60] G. Marchiori,[60] M. Morganti,[60] N. Neri,[60] E. Paoloni,[60] G. Rizzo,[60] J. J. Walsh,[60] J. Biesiada,[61] Y. P. Lau,[61] D. Lopes Pegna,[61] C. Lu,[61] J. Olsen,[61] A. J. S. Smith,[61] A. V. Telnov,[61] E. Baracchini,[62]

1550-7998/2009/79(3)/031102(8)

G. Cavoto,[62] D. del Re,[62] E. Di Marco,[62] R. Faccini,[62] F. Ferrarotto,[62] F. Ferroni,[62] M. Gaspero,[62] P. D. Jackson,[62] L. Li Gioi,[62] M. A. Mazzoni,[62] S. Morganti,[62] G. Piredda,[62] F. Polci,[62] F. Renga,[62] C. Voena,[62] M. Ebert,[63] T. Hartmann,[63] H. Schröder,[63] R. Waldi,[63] T. Adye,[64] B. Franek,[64] E. O. Olaiya,[64] W. Roethel,[64] F. F. Wilson,[64] S. Emery,[65] M. Escalier,[65] L. Esteve,[65] A. Gaidot,[65] S. F. Ganzhur,[65] G. Hamel de Monchenault,[65] W. Kozanecki,[65] G. Vasseur,[65] Ch. Yèche,[65] M. Zito,[65] X. R. Chen,[66] H. Liu,[66] W. Park,[66] M. V. Purohit,[66] R. M. White,[66] J. R. Wilson,[66] M. T. Allen,[67] D. Aston,[67] R. Bartoldus,[67] P. Bechtle,[67] J. F. Benitez,[67] R. Cenci,[67] J. P. Coleman,[67] M. R. Convery,[67] J. C. Dingfelder,[67] J. Dorfan,[67] G. P. Dubois-Felsmann,[67] W. Dunwoodie,[67] R. C. Field,[67] S. J. Gowdy,[67] M. T. Graham,[67] P. Grenier,[67] C. Hast,[67] W. R. Innes,[67] J. Kaminski,[67] M. H. Kelsey,[67] H. Kim,[67] P. Kim,[67] M. L. Kocian,[67] D. W. G. S. Leith,[67] S. Li,[67] B. Lindquist,[67] S. Luitz,[67] V. Luth,[67] H. L. Lynch,[67] D. B. MacFarlane,[67] H. Marsiske,[67] R. Messner,[67] D. R. Muller,[67] H. Neal,[67] S. Nelson,[67] C. P. O'Grady,[67] I. Ofte,[67] A. Perazzo,[67] M. Perl,[67] B. N. Ratcliff,[67] A. Roodman,[67] A. A. Salnikov,[67] R. H. Schindler,[67] J. Schwiening,[67] A. Snyder,[67] D. Su,[67] M. K. Sullivan,[67] K. Suzuki,[67] S. K. Swain,[67] J. M. Thompson,[67] J. Va'vra,[67] A. P. Wagner,[67] M. Weaver,[67] C. A. West,[67] W. J. Wisniewski,[67] M. Wittgen,[67] D. H. Wright,[67] H. W. Wulsin,[67] A. K. Yarritu,[67] K. Yi,[67] C. C. Young,[67] V. Ziegler,[67] P. R. Burchat,[68] A. J. Edwards,[68] S. A. Majewski,[68] T. S. Miyashita,[68] B. A. Petersen,[68] L. Wilden,[68] S. Ahmed,[69] M. S. Alam,[69] R. Bula,[69] J. A. Ernst,[69] B. Pan,[69] M. A. Saeed,[69] S. B. Zain,[69] S. M. Spanier,[70] B. J. Wogsland,[70] R. Eckmann,[71] J. L. Ritchie,[71] A. M. Ruland,[71] C. J. Schilling,[71] R. F. Schwitters,[71] B. W. Drummond,[72] J. M. Izen,[72] X. C. Lou,[72] S. Ye,[72] F. Bianchi,[73] D. Gamba,[73] M. Pelliccioni,[73] M. Bomben,[74] L. Bosisio,[74] C. Cartaro,[74] G. Della Ricca,[74] L. Lanceri,[74] L. Vitale,[74] V. Azzolini,[75] N. Lopez-March,[75] F. Martinez-Vidal,[75] D. A. Milanes,[75] A. Oyanguren,[75] J. Albert,[76] Sw. Banerjee,[76] B. Bhuyan,[76] H. H. F. Choi,[76] K. Hamano,[76] R. Kowalewski,[76] M. J. Lewczuk,[76] I. M. Nugent,[76] J. M. Roney,[76] R. J. Sobie,[76] T. J. Gershon,[77] P. F. Harrison,[77] J. Ilic,[77] T. E. Latham,[77] G. B. Mohanty,[77] H. R. Band,[78] X. Chen,[78] S. Dasu,[78] K. T. Flood,[78] Y. Pan,[78] M. Pierini,[78] R. Prepost,[78] C. O. Vuosalo,[78] and S. L. Wu[78]

(*BaBar* Collaboration)

[1] *Laboratoire de Physique des Particules, IN2P3/CNRS et Université de Savoie, F-74941 Annecy-Le-Vieux, France*
[2] *Universitat de Barcelona, Facultat de Fisica, Departament ECM, E-08028 Barcelona, Spain*
[3] *Università di Bari, Dipartimento di Fisica and INFN, I-70126 Bari, Italy*
[4] *University of Bergen, Institute of Physics, N-5007 Bergen, Norway*
[5] *Lawrence Berkeley National Laboratory and University of California, Berkeley, California 94720, USA*
[6] *University of Birmingham, Birmingham, B15 2TT, United Kingdom*
[7] *Ruhr Universität Bochum, Institut für Experimentalphysik 1, D-44780 Bochum, Germany*
[8] *University of Bristol, Bristol BS8 1TL, United Kingdom*
[9] *University of British Columbia, Vancouver, British Columbia, Canada V6T 1Z1*
[10] *Brunel University, Uxbridge, Middlesex UB8 3PH, United Kingdom*
[11] *Budker Institute of Nuclear Physics, Novosibirsk 630090, Russia*
[12] *University of California at Irvine, Irvine, California 92697, USA*
[13] *University of California at Los Angeles, Los Angeles, California 90024, USA*
[14] *University of California at Riverside, Riverside, California 92521, USA*
[15] *University of California at San Diego, La Jolla, California 92093, USA*
[16] *University of California at Santa Barbara, Santa Barbara, California 93106, USA*
[17] *University of California at Santa Cruz, Institute for Particle Physics, Santa Cruz, California 95064, USA*
[18] *California Institute of Technology, Pasadena, California 91125, USA*
[19] *University of Cincinnati, Cincinnati, Ohio 45221, USA*
[20] *University of Colorado, Boulder, Colorado 80309, USA*
[21] *Colorado State University, Fort Collins, Colorado 80523, USA*
[22] *Universität Dortmund, Institut für Physik, D-44221 Dortmund, Germany*
[23] *Technische Universität Dresden, Institut für Kern- und Teilchenphysik, D-01062 Dresden, Germany*
[24] *Laboratoire Leprince-Ringuet, CNRS/IN2P3, Ecole Polytechnique, F-91128 Palaiseau, France*
[25] *University of Edinburgh, Edinburgh EH9 3JZ, United Kingdom*
[26] *Università di Ferrara, Dipartimento di Fisica and INFN, I-44100 Ferrara, Italy*
[27] *Laboratori Nazionali di Frascati dell'INFN, I-00044 Frascati, Italy*
[28] *Università di Genova, Dipartimento di Fisica and INFN, I-16146 Genova, Italy*
[29] *Harvard University, Cambridge, Massachusetts 02138, USA*
[30] *Universität Heidelberg, Physikalisches Institut, Philosophenweg 12, D-69120 Heidelberg, Germany*
[31] *Imperial College London, London, SW7 2AZ, United Kingdom*
[32] *University of Iowa, Iowa City, Iowa 52242, USA*
[33] *Iowa State University, Ames, Iowa 50011-3160, USA*
[34] *Johns Hopkins University, Baltimore, Maryland 21218, USA*

[35]*Universität Karlsruhe, Institut für Experimentelle Kernphysik, D-76021 Karlsruhe, Germany*
[36]*Laboratoire de l'Accélérateur Linéaire, IN2P3/CNRS et Université Paris-Sud 11,*
Centre Scientifique d'Orsay, B. P. 34, F-91898 ORSAY Cedex, France
[37]*Lawrence Livermore National Laboratory, Livermore, California 94550, USA*
[38]*University of Liverpool, Liverpool L69 7ZE, United Kingdom*
[39]*Queen Mary, University of London, E1 4NS, United Kingdom*
[40]*University of London, Royal Holloway and Bedford New College, Egham, Surrey TW20 0EX, United Kingdom*
[41]*University of Louisville, Louisville, Kentucky 40292, USA*
[42]*University of Manchester, Manchester M13 9PL, United Kingdom*
[43]*University of Maryland, College Park, Maryland 20742, USA*
[44]*University of Massachusetts, Amherst, Massachusetts 01003, USA*
[45]*Massachusetts Institute of Technology, Laboratory for Nuclear Science, Cambridge, Massachusetts 02139, USA*
[46]*McGill University, Montréal, Québec, Canada H3A 2T8*
[47]*Università di Milano, Dipartimento di Fisica and INFN, I-20133 Milano, Italy*
[48]*University of Mississippi, University, Mississippi 38677, USA*
[49]*Université de Montréal, Physique des Particules, Montréal, Québec, Canada H3C 3J7*
[50]*Mount Holyoke College, South Hadley, Massachusetts 01075, USA*
[51]*Università di Napoli Federico II, Dipartimento di Scienze Fisiche and INFN, I-80126, Napoli, Italy*
[52]*NIKHEF, National Institute for Nuclear Physics and High Energy Physics, NL-1009 DB Amsterdam, The Netherlands*
[53]*University of Notre Dame, Notre Dame, Indiana 46556, USA*
[54]*Ohio State University, Columbus, Ohio 43210, USA*
[55]*University of Oregon, Eugene, Oregon 97403, USA*
[56]*Università di Padova, Dipartimento di Fisica and INFN, I-35131 Padova, Italy*
[57]*Laboratoire de Physique Nucléaire et de Hautes Energies, IN2P3/CNRS, Université Pierre et Marie Curie-Paris6,*
Université Denis Diderot-Paris7, F-75252 Paris, France
[58]*University of Pennsylvania, Philadelphia, Pennsylvania 19104, USA*
[59]*Università di Perugia, Dipartimento di Fisica and INFN, I-06100 Perugia, Italy*
[60]*Università di Pisa, Dipartimento di Fisica, Scuola Normale Superiore and INFN, I-56127 Pisa, Italy*
[61]*Princeton University, Princeton, New Jersey 08544, USA*
[62]*Università di Roma La Sapienza, Dipartimento di Fisica and INFN, I-00185 Roma, Italy*
[63]*Universität Rostock, D-18051 Rostock, Germany*
[64]*Rutherford Appleton Laboratory, Chilton, Didcot, Oxon, OX11 0QX, United Kingdom*
[65]*DSM/Dapnia, CEA/Saclay, F-91191 Gif-sur-Yvette, France*
[66]*University of South Carolina, Columbia, South Carolina 29208, USA*
[67]*Stanford Linear Accelerator Center, Stanford, California 94309, USA*
[68]*Stanford University, Stanford, California 94305-4060, USA*
[69]*State University of New York, Albany, New York 12222, USA*
[70]*University of Tennessee, Knoxville, Tennessee 37996, USA*
[71]*University of Texas at Austin, Austin, Texas 78712, USA*
[72]*University of Texas at Dallas, Richardson, Texas 75083, USA*
[73]*Università di Torino, Dipartimento di Fisica Sperimentale and INFN, I-10125 Torino, Italy*
[74]*Università di Trieste, Dipartimento di Fisica and INFN, I-34127 Trieste, Italy*
[75]*IFIC, Universitat de Valencia-CSIC, E-46071 Valencia, Spain*
[76]*University of Victoria, Victoria, British Columbia, Canada V8W 3P6*
[77]*Department of Physics, University of Warwick, Coventry CV4 7AL, United Kingdom*
[78]*University of Wisconsin, Madison, Wisconsin 53706, USA*

(Received 28 April 2008; published 26 February 2009)

We use a sample of 384×10^6 $B\bar{B}$ events collected with the *BABAR* detector at the PEP-II e^+e^- collider to study angular distributions in the rare decays $B \to K^* \ell^+ \ell^-$, where $\ell^+\ell^-$ is either e^+e^- or $\mu^+\mu^-$. For low dilepton invariant masses, $m_{\ell\ell} < 2.5\ \mathrm{GeV}/c^2$, we measure a lepton forward-backward asymmetry $\mathcal{A}_{\mathrm{FB}} = 0.24^{+0.18}_{-0.23} \pm 0.05$ and K^* longitudinal polarization $F_L = 0.35 \pm 0.16 \pm 0.04$. For $m_{\ell\ell} > 3.2\ \mathrm{GeV}/c^2$, we measure $\mathcal{A}_{\mathrm{FB}} = 0.76^{+0.52}_{-0.32} \pm 0.07$ and $F_L = 0.71^{+0.20}_{-0.22} \pm 0.04$.

DOI: 10.1103/PhysRevD.79.031102 PACS numbers: 13.20.He

---

[*]Deceased.

[†]Now at Temple University, Philadelphia, Pennsylvania 19122, USA.

[‡]Now at Tel Aviv University, Tel Aviv, 69978, Israel.

[§]Also with Università di Perugia, Dipartimento di Fisica, Perugia, Italy.

[‖]Also with Universita' di Sassari, Sassari, Italy.

The decays $B \to K^* \ell^+ \ell^-$, where $K^* \to K\pi$ and $\ell^+\ell^-$ is either an e^+e^- or $\mu^+\mu^-$ pair, arise from flavor-changing neutral currents (FCNC), which are forbidden at tree level in the standard model (SM). The lowest-order SM processes contributing to these decays are the photon or Z penguin and the W^+W^- box diagrams shown in Fig. 1. The amplitudes can be expressed in terms of effective Wilson coefficients for the electromagnetic penguin, $C_7^{\rm eff}$, and the vector and axial-vector electroweak contributions, $C_9^{\rm eff}$ and $C_{10}^{\rm eff}$, respectively, arising from the interference of the Z penguin and W^+W^- box diagrams [1]. The angular distributions in these decays as a function of dilepton mass squared $q^2 = m^2_{\ell^+\ell^-}$ are sensitive to many possible new physics contributions [2].

We describe measurements of the distribution of the angle θ_K between the K and the B directions in the K^* rest frame. A fit to $\cos\theta_K$ of the form [3]

$$\tfrac{3}{2} F_L \cos^2\theta_K + \tfrac{3}{4}(1 - F_L)(1 - \cos^2\theta_K) \qquad (1)$$

determines F_L, the K^* longitudinal polarization fraction. We also describe measurements of the distribution of the angle θ_ℓ between the $\ell^+(\ell^-)$ and the $B(\bar{B})$ direction in the $\ell^+\ell^-$ rest frame. A fit to $\cos\theta_\ell$ of the form [3]

$$\tfrac{3}{4} F_L (1 - \cos^2\theta_\ell) + \tfrac{3}{8}(1 - F_L)(1 + \cos^2\theta_\ell) + \mathcal{A}_{\rm FB} \cos\theta_\ell \qquad (2)$$

determines $\mathcal{A}_{\rm FB}$, the lepton forward-backward asymmetry. These measurements are done in a low q^2 region $0.1 < q^2 < 6.25$ GeV$^2/c^4$, and in a high q^2 region above 10.24 GeV$^2/c^4$. We remove the J/ψ and $\psi(2S)$ resonances by vetoing events in the regions $q^2 =$ 6.25–10.24 GeV$^2/c^4$ and $q^2 =$ 12.96–14.06 GeV$^2/c^4$ respectively.

The SM predicts a distinctive variation of $\mathcal{A}_{\rm FB}$ arising from the interference between the different amplitudes. The expected SM dependence of $A_{\rm FB}$ and F_L on q^2 along with variations due to opposite-sign Wilson coefficients are shown in Fig. 3. At low q^2, where $C_7^{\rm eff}$ dominates, $\mathcal{A}_{\rm FB}$ is expected to be small with a zero-crossing point at $q^2 \sim 4$ GeV$^2/c^4$ [4–6]. There is an experimental constraint on the magnitude of $C_7^{\rm eff}$ coming from the branching fraction for $b \to s\gamma$ [6,7], which corresponds to the limit $q^2 \to 0$. However, a reversal of the sign of $C_7^{\rm eff}$ is allowed. At high q^2, the product of $C_9^{\rm eff}$ and $C_{10}^{\rm eff}$ is expected to give a large positive asymmetry. Right-handed weak currents have an opposite-sign $C_9^{\rm eff} C_{10}^{\rm eff}$ which would give a negative $\mathcal{A}_{\rm FB}$ at high q^2. Contributions from non-SM processes can change the magnitudes and relative signs of $C_7^{\rm eff}$, $C_9^{\rm eff}$ and $C_{10}^{\rm eff}$, and may introduce complex phases between them [3,8]. An experimental determination of F_L is required to obtain a model-independent $\mathcal{A}_{\rm FB}$ result, and thus avoid drawing possibly incorrect inferences about new physics from our observations.

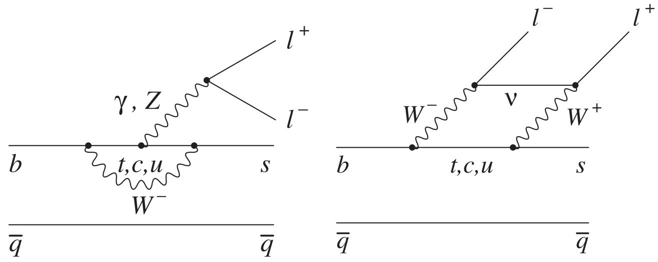

FIG. 1. Lowest-order Feynman diagrams for $b \to s\ell^+\ell^-$.

We reconstruct signal events in six separate flavor-specific final states containing an e^+e^- or $\mu^+\mu^-$ pair, and a $K^*(892)$ candidate reconstructed as $K^+\pi^-$, $K^+\pi^0$ or $K^0_S\pi^+$ (or their charge conjugates). To understand combinatorial backgrounds we also reconstruct samples containing the same hadronic final states and $e^\pm\mu^\mp$ pairs, where no signal is expected because of lepton-flavor conservation. To understand backgrounds from hadrons (h) misidentified as muons, we similarly reconstruct samples containing $h^\pm\mu^\mp$ pairs with no particle identification requirement for the $h^\pm$.

We use a data set of 384×10^6 $B\bar{B}$ pairs collected at the $\Upsilon(4S)$ resonance with the *BABAR* detector [9] at the PEP-II asymmetric-energy e^+e^- collider. Tracking is provided by a five-layer silicon vertex tracker and a 40-layer drift chamber in a 1.5 T magnetic field. We identify electrons with a CsI(Tl) electromagnetic calorimeter, muons with an instrumented magnetic flux return, and K^+ using a detector of internally reflected Cherenkov light as well as ionization energy loss information. Charged tracks other than identified e, μ and K candidates are treated as pions. Electrons (muons) are required to have momenta $p > 0.3(0.7)$ GeV$/c$ in the laboratory frame. We add photons to electrons when they are consistent with bremsstrahlung, and do not use electrons that arise from photon conversions to low-mass e^+e^- pairs. Neutral $K^0_S \to \pi^+\pi^-$ candidates are required to have an invariant mass consistent with the nominal K^0 mass [10], and a flight distance from the e^+e^- interaction point which is more than 3 times its uncertainty. Neutral pion candidates are formed from two photons with $E_\gamma > 50$ MeV, and an invariant mass between 115 and 155 MeV$/c^2$. We require $K^*(892)$ candidates to have an invariant mass $0.82 < M(K\pi) < 0.97$ GeV$/c^2$.

$B \to K^*\ell^+\ell^-$ decays are characterized by the kinematic variables $m_{\rm ES} = \sqrt{s/4 - p_B^{*2}}$ and $\Delta E = E_B^* - \sqrt{s}/2$, where p_B^* and E_B^* are the reconstructed B momentum and energy in the center-of-mass (CM) frame, and $\sqrt{s}$ is the total CM energy. We define a fit region $m_{\rm ES} > 5.2$ GeV$/c^2$, with $-0.07 < \Delta E < 0.04(-0.04 < \Delta E < 0.04)$ GeV for e^+e^- ($\mu^+\mu^-$) final states in the low q^2 region, and $-0.08 < \Delta E < 0.05(-0.05 < \Delta E < 0.05)$ GeV for high q^2. We use the wider (narrower) ΔE windows to select the $e^\pm\mu^\mp$ ($h^\pm\mu^\mp$) background samples.

The most significant background arises from random combinations of leptons from semileptonic B and D decays. In $B\bar{B}$ events the leptons are kinematically correlated if they come from $B \to D^{(*)}\ell\nu$, $D \to K^{(*)}\ell\nu$. Uncorrelated backgrounds combine leptons from separate B decays or from continuum $e^+e^- \to c\bar{c}$ events. We suppress these types of combinatorial background through the use of neural networks (NN). For each final state we use four separate NN designed to suppress either continuum or $B\bar{B}$ backgrounds in either the low or high q^2 regions, and different selections of NN inputs are used depending on q^2 bin (low, high), the identity of the leptons in the final state (e, μ), and the type of background ($B\bar{B}$, continuum). Inputs include:

(i) event thrust;
(ii) ratio of second-to-zeroth Fox-Wolfram moments [11];
(iii) $m_{\rm ES}$ and ΔE of the rest of the event (ROE), comprising all charged tracks and neutral energy deposits not used to reconstruct the signal candidate;
(iv) the magnitude of the total event transverse momentum, which is correlated with missing energy due to unreconstructed neutrinos in background semileptonic decays;
(v) dilepton system's distance of closest approach along the beam axis, and separately in the plane perpendicular to the beam axis, to the primary interaction point;
(vi) vertex probability of the signal candidate and, separately, of the dilepton system;
(vii) the cosines in the CM frame of the angle between the B candidate's momentum and the beam axis, the angle between the event thrust axis and the beam axis ($\theta_{\rm thrust}$), the angle between the ROE thrust axis and the beam axis ($\theta_{\rm thrust}^{\rm ROE}$), and the angle between $\theta_{\rm thrust}^{\rm ROE}$ and $\theta_{\rm thrust}$.

There is also a background contribution in the signal region from $B \to D(K^*\pi)\pi$ decays, where both pions are misidentified. The misidentification rates for muons and electrons are ~2% and ~0.1%, respectively, so this background is only significant in the $\mu^+\mu^-$ final states. These events are vetoed if the invariant mass of the $K^*\pi$ system is in the range 1.84–1.90 GeV/c^2.

We optimize the NN and ΔE selections for each final state in each q^2 bin to give the best combined statistical signal significance in the $m_{\rm ES}$ signal region $m_{\rm ES} > 5.27$ GeV/c^2 for the sum of all six final states. After all these selections have been applied, the final reconstruction efficiencies and expected yields for signal events (calculated using world average branching fractions [7]), as well as expected yields for background events in the signal region, are shown in Table I.

TABLE I. Signal efficiencies (%), and expected signal and background yields for $m_{\rm ES} > 5.27$ GeV/c^2, for low and high q^2 regions.

	Signal Eff.		Signal Yield		Bkgd. Yield	
Mode	low	high	low	high	low	high
$K^+\pi^0\mu^+\mu^-$	1.6	3.1	1.0	1.8	0.7	3.8
$K_S^0\pi^+\mu^+\mu^-$	3.6	5.5	3.0	4.5	0.3	1.4
$K^+\pi^-\mu^+\mu^-$	4.5	8.1	5.5	9.6	0.0	3.1
$K^+\pi^0e^+e^-$	4.6	5.3	2.8	3.1	1.7	2.4
$K_S^0\pi^+e^+e^-$	7.0	5.4	5.9	4.4	0.3	1.4
$K^+\pi^-e^+e^-$	8.6	10.3	10.5	12.2	1.7	2.4
Total Yield			28.6	35.8	4.8	14.5

For each q^2 region, we combine events from all six final states and perform three successive unbinned maximum likelihood fits. Because of the relatively small number of signal candidates in each q^2 region, a simultaneous fit over $m_{\rm ES}$, $\cos\theta_K$, and $\cos\theta_\ell$ is unlikely to converge and a sequential fitting procedure is required. We initially fit the $m_{\rm ES}$ distribution using events with $m_{\rm ES} > 5.2$ GeV/c^2 to obtain the signal and background yields, N_S and N_B, respectively. We use an ARGUS shape [12] with a free shape parameter to describe the combinatorial background in this fit. For the signal, we use a Gaussian shape with a mean $m_{\rm ES} = 5.2791 \pm 0.0001$ GeV/c^2 and $\sigma = 2.60 \pm 0.03$ MeV/c^2, which are determined from a fit to the vetoed charmonium samples. In this and subsequent fits we account for a small contribution from misidentified hadrons by subtracting the $K^*h^\pm\mu^\mp$ events, weighted by the probability for the $h^\pm$ to be misidentified as a muon. We also account in all fits for charmonium events that escape the veto, and for misreconstructed signal events. We estimate contributions from nonresonant $K\pi$ decays by fitting events outside the K^* mass window in the range 0.7–1.1 GeV/c^2. We find no signal-like events that are not accounted for by the tails of the resonant mass distribution, and thus do not expect any significant contribution from nonresonant events within the mass window.

The second fit is to the cosine of the helicity angle of the K^* decay, $\cos\theta_K$, for events with $m_{\rm ES} > 5.27$ GeV/c^2. In this fit, the only free parameter is F_L, with the normalizations for signal and combinatorial background events taken from the initial $m_{\rm ES}$ fit. The background normalization is obtained by integrating, for $m_{\rm ES} > 5.27$ GeV/c^2, the ARGUS shape resulting from the $m_{\rm ES}$ fit. We model the $\cos\theta_K$ shape of the combinatorial background using e^+e^- and $\mu^+\mu^-$ events, as well as lepton-flavor violating $e^+\mu^-$ and μ^+e^- events, in the $5.20 < m_{\rm ES} < 5.27$ GeV/c^2 sideband. The signal distribution given in Eq. (1) is folded with the detector acceptance as a function of $\cos\theta_K$, which is obtained from simulated signal events.

The final fit is to the cosine of the lepton helicity angle, $\cos\theta_\ell$, for events with $m_{\rm ES} > 5.27$ GeV/c^2. The only free parameter in this fit is $\mathcal{A}_{\rm FB}$, with the signal distribution given in Eq. (2) folded with the detector acceptance as a function of $\cos\theta_\ell$. In this fit, the value of F_L is fixed from the result of the second fit, and normalizations for signal and combinatorial background events are identical to those used in the second fit. We constrain the $\cos\theta_\ell$ shape of the

TABLE II. Results for the $B \to J/\psi K^*$ control samples. ΔBF are the differences between the measured branching fractions and the world average value [10]. The previously measured $F_L = 0.56 \pm 0.01$ [13], and the expected $\mathcal{A}_{FB} = 0$.

Mode	ΔBF (10^{-3})	F_L	$\mathcal{A}_{FB}$
$K^+\pi^0\mu^+\mu^-$	$+0.09 \pm 0.12$	0.54 ± 0.03	-0.04 ± 0.05
$K^0_S\pi^+\mu^+\mu^-$	$+0.02 \pm 0.11$	0.55 ± 0.02	$+0.00 \pm 0.05$
$K^+\pi^-\mu^+\mu^-$	-0.03 ± 0.07	0.56 ± 0.02	-0.02 ± 0.02
$K^+\pi^0 e^+e^-$	$+0.16 \pm 0.10$	0.54 ± 0.03	$+0.02 \pm 0.03$
$K^0_S\pi^+ e^+e^-$	$+0.07 \pm 0.10$	0.55 ± 0.02	-0.02 ± 0.04
$K^+\pi^- e^+e^-$	$+0.02 \pm 0.07$	0.56 ± 0.02	$+0.01 \pm 0.02$

TABLE IV. Systematic errors on the measurements of F_L and $\mathcal{A}_{FB}$ in the $K^*\ell^+\ell^-$ samples.

Source of error	F_L		$\mathcal{A}_{FB}$	
	low q^2	high q^2	low q^2	high q^2
m_{ES} fit yields	0.001	0.016	0.003	0.002
F_L fit error			0.025	0.022
Background shape	0.011	0.008	0.017	0.021
Signal model	0.036	0.034	0.030	0.038
Fit bias	0.012	0.020	0.023	0.052
Misreconstructed signal	0.010	0.010	0.020	0.020
Total	0.041	0.044	0.052	0.074

combinatorial background using the same sideband samples as for the $\cos\theta_K$ fit. The correlated leptons from $B \to D^{(*)}\ell\nu$, $D \to K^{(*)}\ell\nu$ give rise to an m_{ES}-dependent peak in the combinatorial background at $\cos\theta_\ell > 0.7$, and we consider this correlation in our study of systematic errors. No such correlation is observed for $\cos\theta_K$.

We test our fits using the large sample of vetoed charmonium events. The branching fractions (BF) and K^* polarization for $B \to J/\psi K^*$ are well known [10,13], and $\mathcal{A}_{FB}$ is expected to be zero. The results of the fits to the six final states are all consistent with expected values (see Table II). We further test our methodology by performing the m_{ES} and $\cos\theta_\ell$ fits on a sample of $B^+ \to K^+\ell^+\ell^-$ decays. The results are given in Table III and are consistent with negligible forward-backward asymmetry, as expected in the SM and most new physics models [14].

We validate the fit model by performing ensembles of fits to datasets with events drawn from simulated signal and background event samples. The input SM values of F_L and $\mathcal{A}_{FB}$ are reproduced with the expected statistical errors. A few percent of the fits do not converge due to small signal yields. We have also performed fits using signal events generated with widely varying values of $C_7^{\rm eff}$, $C_9^{\rm eff}$, and $C_{10}^{\rm eff}$ covering the physically allowed regions of F_L and $\mathcal{A}_{FB}$, and find minimal bias in our fits.

The systematic errors on the fitted values of F_L and $\mathcal{A}_{FB}$ are summarized in Table IV. The uncertainties in the fitted signal yields N_S, due to variations in the ARGUS shape in the m_{ES} fits, are propagated into the angular fits. The errors on the fitted F_L values are propagated into the $\mathcal{A}_{FB}$ fits. We vary the combinatorial background shapes by dividing the sideband sample into two disjoint regions in m_{ES}. We vary the signal model using simulated events generated with different form factors [5,15], and with a range of values of $C_7^{\rm eff}$, $C_9^{\rm eff}$, and $C_{10}^{\rm eff}$, to determine an average fit bias. Finally, the modeling of misreconstructed signal events is constrained by the fits to the charmonium samples (Table II), where it is the largest systematic uncertainty.

TABLE III. Results for the fits to the $K\ell^+\ell^-$ and $K^*\ell^+\ell^-$ samples. N_S is the number of signal events in the m_{ES} fit. The quoted errors are statistical only.

Decay	q^2	N_S	F_L	$\mathcal{A}_{FB}$
$K\ell^+\ell^-$	low	26.0 ± 5.7		$+0.04^{+0.16}_{-0.24}$
	high	26.5 ± 6.7		$+0.20^{+0.14}_{-0.22}$
$K^*\ell^+\ell^-$	low	27.2 ± 6.3	0.35 ± 0.16	$+0.24^{+0.18}_{-0.23}$
	high	36.6 ± 9.6	$0.71^{+0.20}_{-0.22}$	$+0.76^{+0.52}_{-0.32}$

The final fits to the $K^*\ell^+\ell^-$ samples are shown in Fig. 2. The results for F_L and $\mathcal{A}_{FB}$ are given in Table III and are shown in Fig. 3. In the low q^2 region, where we expect

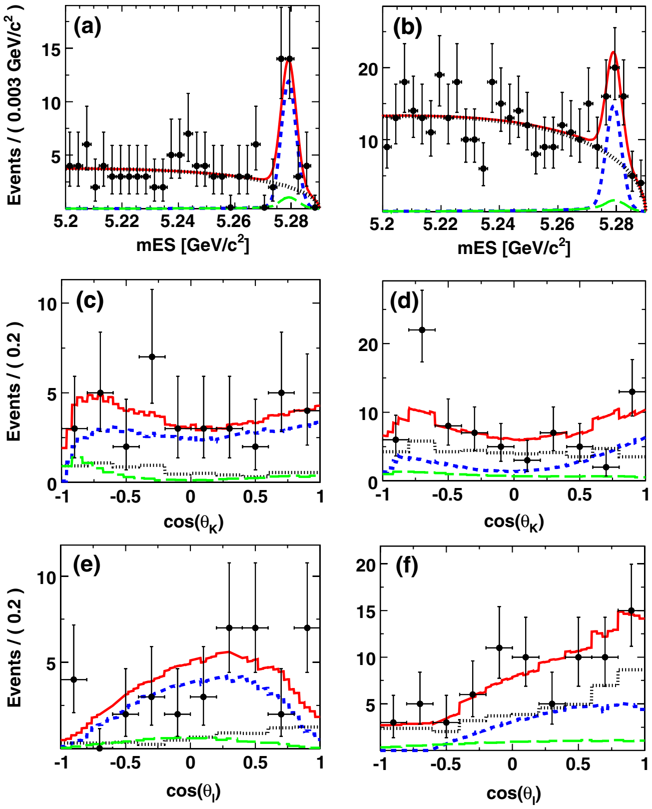

FIG. 2 (color online). $K^*\ell^+\ell^-$ fits: (a) low q^2 m_{ES}, (b) high q^2 m_{ES}, (c) low q^2 $\cos\theta_K$, (d) high q^2 $\cos\theta_K$, (e) low q^2 $\cos\theta_\ell$, (f) high q^2 $\cos\theta_\ell$; with combinatorial (dotted line) and peaking (long dashed line) background, signal (short dashed line) and total (solid line) fit distributions superimposed on the data points.

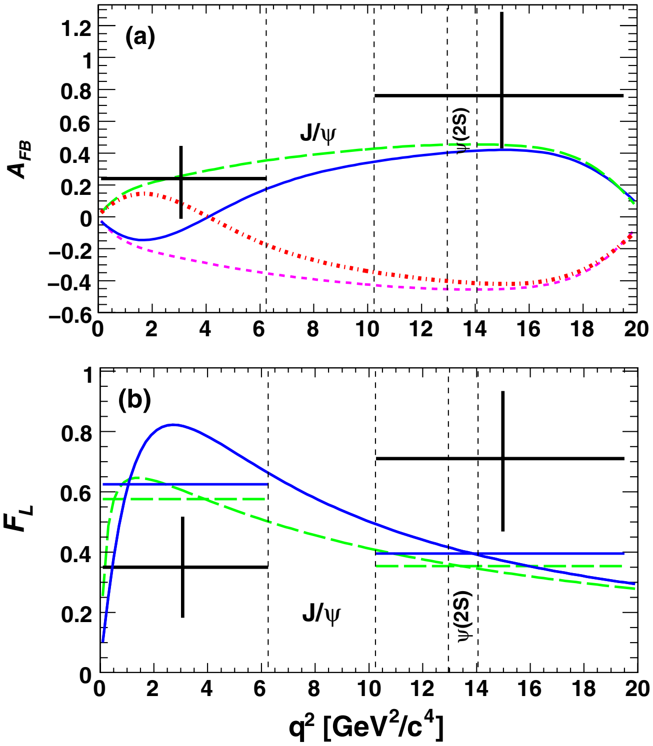

FIG. 3 (color online). Plots of our results for (a) $\mathcal{A}_{\rm FB}$ and (b) F_L for the decay $B \to K^* \ell^+ \ell^-$ showing comparisons with SM (solid line); $C_7^{\rm eff} = -C_7^{\rm eff}$ (long dashed line); $C_9^{\rm eff} C_{10}^{\rm eff} = -C_9^{\rm eff} C_{10}^{\rm eff}$ (short dashed line); $C_7^{\rm eff} = -C_7^{\rm eff}$, $C_9^{\rm eff} C_{10}^{\rm eff} = -C_9^{\rm eff} C_{10}^{\rm eff}$ (dash-dotted line). Statistical and systematic errors are added in quadrature. Expected F_L values integrated over each q^2 region are also shown. The F_L curves with $C_9^{\rm eff} C^{\rm eff} = -C_9^{\rm eff} C_{10}^{\rm eff}$ are nearly identical to the two curves shown.

$\mathcal{A}_{\rm FB} \sim -0.03$ and $F_L \sim 0.63$ from the SM, we measure $\mathcal{A}_{\rm FB} = 0.24^{+0.18}_{-0.23} \pm 0.05$ and $F_L = 0.35 \pm 0.16 \pm 0.04$, where the first error is statistical and the second is systematic. In the high q^2 region, the SM expectation is $\mathcal{A}_{\rm FB} \sim 0.38$ and $F_L \sim 0.40$, and we measure $\mathcal{A}_{\rm FB} = 0.76^{+0.52}_{-0.32} \pm 0.07$ and $F_L = 0.71^{+0.20}_{-0.22} \pm 0.04$, with a signal yield of 36.6 ± 9.6 events. Theoretical uncertainties on the expected SM F_L and $\mathcal{A}_{\rm FB}$ values are generally difficult to characterize in the high q^2 region, and although under better control for $1 < q^2 < 6$ GeV$^2/c^4$, the extension of our low q^2 region below 1 GeV$^2/c^4$ makes estimates of uncertainties there difficult also. The quoted values are obtained using our implementation of the physics models described in [4,15], corresponding to the SM curves in Fig. 3.

The expected SM value of $C_{10}^{\rm eff}$ at next-to-next-to-leading logarithmic (NNLL) order is $C_{10}^{\rm eff} = -4.43$ [16]. A more recent NNLL calculation which evaluates contributions from the full set of seven form factors gives $C_{10}^{\rm eff} = -4.13$ [17]. The magnitude of possible contributions from new physics to C_{10} can be constrained if $\mathcal{A}_{\rm FB} > 0$ at high q^2. By combining such a constraint on $\mathcal{A}_{\rm FB}$ with inclusive $b \to s \ell^+ \ell^-$ branching fraction results, an upper bound of $|C_{10}^{\rm NP}| \lesssim 7$ can be obtained, improving on an upper bound derived solely from branching fraction results of $|C_{10}^{\rm NP}| \lesssim 10$ [18]. Our results are consistent with measurements by Belle [19], and replace the earlier *BABAR* results in which only a lower limit on $\mathcal{A}_{\rm FB}$ was set in the low q^2 region [20].

We are grateful for the excellent luminosity and machine conditions provided by our PEP-II colleagues, and for the substantial dedicated effort from the computing organizations that support *BABAR*. The collaborating institutions wish to thank SLAC for its support and kind hospitality. This work is supported by DOE and NSF (USA), NSERC (Canada), CEA and CNRS-IN2P3 (France), BMBF and DFG (Germany), INFN (Italy), FOM (The Netherlands), NFR (Norway), MES (Russia), MEC (Spain), and STFC (United Kingdom). Individuals have received support from the Marie Curie EIF (European Union) and the A. P. Sloan Foundation.

---

[1] G. Buchalla, A. J. Buras, and M. E. Lautenbacher, Rev. Mod. Phys. **68**, 1125 (1996).
[2] G. Burdman, Phys. Rev. D **52**, 6400 (1995); J. L. Hewett and J. D. Wells, Phys. Rev. D **55**, 5549 (1997); T. Feldmann and J. Matias, J. High Energy Phys. 01 (2003) 074; W. J. Li, Y. B. Dai, and C. S. Huang, Eur. Phys. J. C **40**, 565 (2005); Y. G. Xu, R. M. Wang, and Y. D. Yang, Phys. Rev. D **74**, 114019 (2006); P. Colangelo, F. De Fazio, R. Ferrandes, and T. N. Pham, Phys. Rev. D **73**, 115006 (2006).
[3] F. Kruger and J. Matias, Phys. Rev. D **71**, 094009 (2005).
[4] A. Ali, P. Ball, L. T. Handoko, and G. Hiller, Phys. Rev. D **61**, 074024 (2000).
[5] F. Kruger, L. M. Sehgal, N. Sinha, and R. Sinha, Phys. Rev. D **61**, 114028 (2000); **63**, 019901(E) (2001); A. Ali, E. Lunghi, C. Greub, and G. Hiller, Phys. Rev. D **66**, 034002 (2002); K. S. M. Lee, Z. Ligeti, I. W. Stewart, and F. J. Tackmann, Phys. Rev. D **75**, 034016 (2007).
[6] M. Beneke, T. Feldmann, and D. Seidel, Nucl. Phys. **B612**, 25 (2001).
[7] E. Barberio *et al.* (Heavy Flavor Averaging Group (HFAG) Collaboration), arXiv:0704.3575; C. Bobeth, M. Bona, A. J. Buras, T. Ewerth, M. Pierini, L. Silvestrini, and A. Weiler, Nucl. Phys. **B726**, 252 (2005).
[8] A. Hovhannisyan, W. S. Hou, and N. Mahajan, Phys. Rev. D **77**, 014016 (2008).
[9] B. Aubert *et al.* (*BABAR* Collaboration), Nucl. Instrum. Methods Phys. Res., Sect. A **479**, 1 (2002).

[10] W. M. Yao *et al.* (Particle Data Group), J. Phys. G **33**, 1 (2006).
[11] G. C. Fox and S. Wolfram, Nucl. Phys. **B149**, 413 (1979); **B157**, 543(E) (1979).
[12] H. Albrecht *et al.* (ARGUS Collaboration), Z. Phys. C **48**, 543 (1990).
[13] B. Aubert *et al.* (*BABAR* Collaboration), Phys. Rev. D **76**, 031102 (2007).
[14] C. Bobeth, G. Hiller, and G. Piranishvili, J. High Energy Phys. 12 (2007) 040.
[15] P. Ball and R. Zwicky, Phys. Rev. D **71**, 014029 (2005).
[16] M. Beneke, T. Feldmann, and D. Seidel, Eur. Phys. J. C **41**, 173 (2005).
[17] W. Altmannshofer, P. Ball, A. Bharucha, A. J. Buras, D. M. Straub, and M. Wick, J. High Energy Phys. 01 (2009) 019.
[18] C. Bobeth, G. Hiller, and G. Piranishvili, J. High Energy Phys. 07 (2008) 106.
[19] A. Ishikawa *et al.*, Phys. Rev. Lett. **96**, 251801 (2006).
[20] B. Aubert *et al.* (*BABAR* Collaboration), Phys. Rev. D **73**, 092001 (2006).